



UNIVERSITI PUTRA MALAYSIA

**SYNTHESIS, CHARACTERIZATION AND APPLICATION OF
CARBON NANOTUBES AND CARBON NANOFIBERS**

MUATAZ ALI ATIEH HUSSEIN.

FK 2005 25

**SYNTHESIS, CHARACTERIZATION AND APPLICATION OF
CARBON NANOTUBES AND CARBON NANOFIBERS**

By

MUATAZ ALI ATIEH HUSSIEN

**Thesis Submitted to the School of Graduate Studies, Universiti
Putra Malaysia, in Fulfilment of the Requirements for the Degree
of Doctor of Philosophy**

May 2005



بِسْمِ اللَّهِ الرَّحْمَنِ الرَّحِيمِ

اقْرَأْ بِاسْمِ رَبِّكَ الَّذِي خَلَقَ (1)

خَلَقَ الْإِنْسَانَ مِنْ عَلَقٍ (2)

اقْرَأْ وَرَبُّكَ الْأَكْرَمُ (3)

الَّذِي عَلَّمَ بِالْقَلَمِ (4)

عَلَّمَ الْإِنْسَانَ مَا لَمْ يَعْلَمِ (5)

Abstract of thesis presented to the Senate of Universiti Putra
Malaysia in fulfilment of the requirement for the degree of Doctor of
Philosophy

**SYNTHESIS, CHARACTERIZATION AND APPLICATION OF
CARBON NANOTUBES AND CARBON NANOFIBERS**

By

MUATAZ ALI ATIEH HUSSIEN

May 2005

Chairman : Associate Professor Fakhru'l-Razi Ahmadun, PhD

Faculty : Engineering

Well aligned multi wall carbon nanotubes (MWCNTs), carbon nanofibers (CNFs) and other type of carbon nanostructure materials have been synthesized by a fabricated floating catalyst chemical vapor deposition (FC-CVD) method. This involved the pyrolysis of benzene-ferrocene vapor mixture. The CVD parameters (Hydrogen flow rate, reaction time and reaction temperature) were studied to selectively synthesize nanotubes and nanofibers with required dimensions. Carbon nanotubes films with a diameter of 2-50 nm and nanofiber with a diameter range from 100-300 nm were synthesized in a benzene/hydrogen atmosphere. Furthermore vapor grown carbon fibers have been synthesized with different diameters and lengths. Iron clusters that were produced from the thermal decomposition of ferrocene films were used as catalyst for the synthesis of the carbon structures.



The effects of different hydrogen flow rates (50-500 ml/min) on the morphology, quality and quantity of the product were investigated. Maximum yield and purity was obtained at 300 ml/min.

The effect of the reaction time on the purity and yield of carbon nanotubes was studied from 1 minute to 60 minutes. There was no effect of the reaction time on the average diameter while maximum yield of carbon nanotubes was achieved at 45 minutes.

The last variable was the reaction temperature, which was varied from 500 °C to 1200 °C. By controlling the growth temperature, carbon nanotubes (CNTs), carbon nanofibers (CNFs) and vapor grown carbon fiber with different structures were produced. Increasing the temperature has a remarkable effect on the size and shape of the catalyst and this in turn affected the diameter distribution and structure of the carbon materials. The carbon nanotubes were produced from 600 °C to 850 °C with maximum yield at 850 °C, while for the production of carbon nanofibers the reaction temperature was from 900 °C to 1000 °C with a maximum yield at 1000 °C. Vapor grown carbon fibers were produced at 1050 °C to 1200 °C with maximum yield at 1050 °C.

The synthesised nanotubes/nanofibers were investigated by scanning electron microscopy (SEM) and transmission electron microscopy (TEM).

The thermal degradation kinetics of CNTs was investigated by dynamic thermogravimetry, in an air atmosphere, over the temperature range 25 - 800 °C and at constant nominal heating rate 10 °C/min. The corresponding activation energies, frequency factors and reaction orders were determined.

Homogenous distribution of MWCNTs/CNFs in natural rubber (NR) was achieved by ultrasonic assisted solution-evaporating method. Addition of 1-10 wt% of CNFs and CNTs to natural rubber as nanocomposite increased the rubber mechanical properties significantly. The properties of the composites such as tensile strength, tensile modulus, and elongation at break were studied. In addition to mechanical testing, the dispersion state of the MWNTs into NR was studied by TEM in order to understand the morphology of the resulting system. The result indicated that, by increasing the amount of CNTs and CNFs into the natural rubber the ductility decreased and the material became stronger and tougher but at the same time more brittle. The results showed that by adding 1 wt% of CNTs and CNFs to NR the stress level were increased sharply to 0.56413 and 0.54 MPa respectively compared to NR which was 0.2839 MPa. At 10 wt% the stress level of CNTs with NR were increased sharply 9 times and reached to 2.55 MPa while for CNFs it increased 4.66 times and reached to 1.33 MPa.

Abstrak tesis yang dikemukakan kepada Senat Universiti Putra Malaysia sebagai memenuhi keperluan untuk ijazah Doktor Falsafah

**PENGHASILAN, PENCIRIAN DAN APLIKASI KARBON NANOTIUB
DAN KARBON NANOSERAT.**

Oleh

MUATAZ ALI ATIEH HUSSIEN

Mei 2005

Pengerusi : Profesor Madya Fakhru'l-Razi Ahmadun, PhD

Fakulti : Kejuruteraan

Karbon nanotiub, karbon nanoserat dan struktur karbon yang lain telah disintesis dengan menggunakan kaedah pemangkin terapung-penguraian wap kimia, floating catalyst chemical vapor deposition (FC-CVD) iaitu penguraian benzena dan ferrosin menjadi campuran wap. Parameter CVD (kadar alir hidrogen, masa dan suhu tindak balas) dikaji untuk mendapatkan kaedah penghasilan nanotiub dan nanoserat mengikut dimensi yang dikehendaki. Filem nanotiub dengan julat diameter antara 2–50 nm dan nanoserat antara 100–300 nm disintesis dalam atmosfera benzena/hidrogen. Selain itu, karbon serat turut dihasilkan dengan diameter dan panjang yang berlainan. Kelompok ferum yang terhasil daripada penguraian haba filem ferrosin digunakan sebagai pemangkin bagi menghasilkan struktur karbon.

Kesan kadar alir hidrogen yang berbeza (50-500 ml/min) terhadap morfologi, kualiti dan kuantiti produk turut dikaji. Hasil yang maksimum dan ketulenan yang tinggi diperoleh pada kadar alir hidrogen 300 ml/min.

Pengaruh bagi masa tindak balas terhadap ketulenan dan hasil karbon nanotub dikaji antara satu minit sehingga satu jam. Masa tindak balas tidak memberi kesan terhadap purata diameter sementara hasil maksimum bagi karbon nanotub diperoleh dengan masa tindak balas selama 45 minit.

Pemboleh ubah yang terakhir ialah suhu tindak balas yang dipelbagaikan bermula dari suhu 500 °C hingga 1200 °C. Dengan mengawal suhu tindak balas, nanotub, nanoserat karbon serat dengan struktur yang berbeza dapat dihasilkan. Peningkatan suhu memberi kesan yang besar terhadap saiz. Bentuk pemangkin pula memberi kesan terhadap taburan diameter dan struktur bahan karbon. Karbon nanotub dihasilkan antara suhu 600 °C – 850 °C dengan hasil maksimum pada 850 °C, manakala karbon nanoserat pada suhu antara 900 °C -1000 °C dengan hasil maksimum pada 1000 °C. Karbon serat dihasilkan antara julat suhu 1050 °C -1200 °C dengan hasil maksimum pada suhu 1050 °C.

Morfologi nanotub/nanoserat yang telah dihasilkan kemudiannya dikaji dengan menggunakan Microskop Biasan Elektron, dan Microskop Pancaran Elektron.

Kinetik penguraian haba bagi karbon nanotub dikaji dengan menggunakan termogravimetri dinamik. Pada keadaan udara atmosfera, dengan julat suhu antara 25-800 °C dan kadar pemanasan tetap nominal 10 °C/min, tenaga pengaktifan, faktor frekuensi dan tertib tindak balas yang berkaitan dicari.

Campuran yang sekata antara nanotub/nanoserat dalam getah asli dapat dilakukan dengan menggunakan ultrasonik dengan menggunakan kaedah pemeluwapan larutan. Tambahan nanotub/nanoserat sebanyak 1-10 wt % megikut peratusan berat ke dalam getah asli sebagai nanokomposit telah meningkatkan sifat mekanikal getah tersebut dengan ketara. Sifat-sifat komposit seperti kekuatan regangan, modulus regangan dan pemanjangan pada titik putus dikaji. Selain itu, taburan nanotub dalam getah asli turut dikaji dengan menggunakan Mikroskop Pancaran Elektron, Transmission Electron Microscopy (TEM) untuk lebih memahami morfologi nanokomposit tersebut.

ACKNOWLEDGEMENTS

In The Name of ALLAH, The Most Merciful and Most Beneficent

I am very deeply grateful to ALLAH "S.W" for giving me the opportunity to study with strength and patience to complete this study.

I would like to express my gratitude to my advisor, Associate Prof. Dr. Fakhru'l-Razi Ahmadun for his guidance and encouragement throughout this work. His generosity, patience and sense of humour have always been admired. Many thanks go to. Dr. El-Sadiq Mahdi and Dr. Chuah Teong Guan (Lukman AL-Hakeem) for serving as my committee members. I would like to express my most sincere and warmest gratitude to my father Haj Ali Atieh Hussien (Allah reward him, Allah bless him, Allah protect him and Allah give him the heaven), mother (Allah reward her, Allah bless her, Allah protect her and Allah give her the heaven), brothers, sister and my wife for their prayers, loving, generous and moral support during my study.



I certify that an Examination Committee met on 16th September 2005 to conduct the final examination of Muataz Ali Atieh Hussein on his Doctor of Philosophy thesis entitled "Synthesis, Characterization and Application of Carbon Nanotubes and Carbon Nanofibers" in accordance with Universiti Pertanian Malaysia (Higher Degree) Act 1980 and Universiti Pertanian Malaysia (Higher Degree) Regulations 1981. The Committee recommends that the candidate be awarded the relevant degree. Members of the Examination Committee are as follows:

Azni Idris, PhD

Professor
Faculty of Engineering
Universiti Putra Malaysia
(Chairman)

Thomas Choong Shean Yaw, PhD

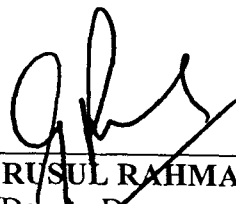
Lecturer
Faculty of Engineering
Universiti Putra Malaysia
(Internal Examiner)

Robiah Yunus, PhD

Associate Professor
Faculty of Engineering
Universiti Putra Malaysia
(Internal Examiner)

Ahmad Fauzi Ismail, PhD

Professor
Faculty of Chemical and Natural Resource Engineering
Universiti Teknologi Malaysia
(External Examiner)



GULAM RUSUL RAHMAT ALI, PhD
Professor/Deputy Dean
School of Graduate Studies
Universiti Putra Malaysia

Date: 25 OCT 2005

This thesis submitted to the Senate of Universiti Putra Malaysia and has been accepted as fulfilment of the requirement for the degree of Doctor of Philosophy. The members of the Supervisory Committee are as follows:

Fakhru'l-Razi Ahmadun, PhD


Associate Professor
Faculty of Engineering
Universiti Putra Malaysia
(Chairman)

Chuah Teong Guan, PhD

Lecturer
Faculty of Engineering
Universiti Putra Malaysia
(Member)

EL-Sadiq Mahdi, PhD

Lecturer
Faculty of Engineering
Universiti Putra Malaysia
(Member)



AINI IDERIS, PhD
Professor/Dean
School of Graduate Studies
Universiti Putra Malaysia

Date: 17 NOV 2005

DECLARATION

I hereby declare that the thesis is based on my original work except for quotations and citation, which have been duly acknowledged. I also declare that it has not been previously or concurrently submitted for any other degree at UPM or other institutions.



MUATAZ ALI ATIEH HUSSEIN

Date: 14 / 10 / 05

TABLE OF CONTENTS

	Page
DEDICATION	ii
ABSTRACT	iii
ABSTRAK	vi
ACKNOWLEDGEMENTS	ix
APPROVAL	x
DECLARATION	xii
LIST OF TABLES	xvi
LIST OF FIGURES	xvii
LIST OF ABBREVIATIONS	xxv
 CHAPTER	
 1 INTRODUCTION	 1
1.1 Problem Statement	4
1.2 Significant of Study	5
1.3 Scope of Study	6
1.4 Objective of Study	7
 2 LITERATURE REVIEW	 8
2.1 History of Carbon Nanotube	8
2.2 Structure of Carbon Nanotube	9
2.3 Properties of Carbon Nanotubes	16
2.3.1 Electronic Properties.	17
2.3.2 Mechanical Properties.	19
2.4 Carbon Nanofibers	21
2.5 Production Methods of Carbon Nanotubes and Carbon Nanofibers	25
2.5.1 Arc-Discharge	26
2.5.2 Laser Ablation	28
2.5.3 Chemical Vapour Deposition (CVD)	30
2.6 Applications of Carbon Nanotubes	50
2.6.1 Nanotube as Composites	50
2.6.2 Field Effect Transistors	67
2.6.3 Field Emission Display (FED)	70
2.6.4 Nanotube Sensors	73
2.6.5 Carbon Nanotube in Microscopy	78
2.6.6 Hydrogen Storage	80
 3 MATERIALS AND METHODS	 84
3.1 Design of a Modified Floating Catalyst Chemical Vapour Deposition (FC-CVD)	84
	xiii

3.2	Fabrication of FC-CVD	87
3.3	Materials	88
3.3.1	Gases	88
3.3.2	Chemicals	88
3.4	Production of Carbon Nanotubes s, Nanofibers and Vapor Growth Carbon Fiber	88
3.5	Calculation of Yield	89
3.6	Characterization	91
3.6.1	Scanning Electron Microscopy (SEM)	92
3.6.2	Transmission Electron Microscopy (TEM)	93
3.6.3	Thermogravimetric Analysis (TGA)	94
3.6.4	Purity Measurement	96
3.7	Application of Carbon Nanotubes and Nanofibers	95
3.7.1	Sample Preparation	96
3.7.2	Mechanical Test	97
3.8	Preparation of Nanofiller/Rubber	98
4	RESULTS AND DISCUSSIONS	101
	Introduction	101
4.1	Effect of hydrogen flow	102
4.1.1	Effect of Hydrogen Flow Rate on the Diameter Distribution of Nanotubes.	102
4.1.2	Effect of Hydrogen Flow Rate on the Purity of CNTs.	110
4.1.3	Effect of Hydrogen Flow Rate on the Carbon Depositions.	114
4.1.4	Effect of Hydrogen Flow Rate on the Yield of Carbon Nanotubes	115
4.1.6	SEM Observations	117
4.1.7	TEM Observations	119
4.1.8	The Role of Hydrogen Flow Rate	122
4.2	Effect or Reaction Time	126
4.2.1	Effect or Reaction Time on the Average Diameter of CNTs	126
4.2.2	Effect of Reaction Time on the Carbon Depositions	127
4.2.3	Effect of Reaction Time on the Yield of Carbon Nanotubes	128
4.3	Effect or Reaction Temperature	129
4.3.1	Effect of Reaction Temperature on Production of Carbon Material.	130
4.3.2	Effect Reaction Temperature on the Purity of CNTs, CNFs and VGCFs.	136
4.3.3	Effect of Reaction Temperature on the Carbon Depositions	138
4.3.4	Effect of Reaction Temperature on the	139

	Yield of Carbon Materials	
4.3.5	SEM Observation	141
4.3.6	TEM Observation	150
4.3.7	The Role of Reaction Temperature	153
4.4	Structures of Carbon Nanotube	157
4.5	Thermal Oxidization Kinetic of Carbon Nanotubes (CNTs).	158
4.5.1	Kinetic theory of carbon nanotubes	159
4.6	Carbon Nanotube and Carbon Nanofiber as Nanocomposite	165
4.6.1	Introduction	165
4.6.2	Effect of Carbon Nanotube on the Mechanical Properties of Natural Rubber.	165
4.6.3	Effect of Carbon Nanofiber on the Mechanical Properties of Natural Rubber.	176
5	CONCLUSION AND RECOMMENDATIONS	185
	REFERENCES	189
	BIODATA OF THE AUTHOR	210

LIST OF TABLES

Table		Page
2.6	Some of the hydrogen storage reported, up to 2001	82
4.1	A summary of the kinetics parameters obtained for thermal oxidization of CNTs	163

LIST OF FIGURES

Figure	Page
2.1 World of carbon related materials	9
2.2 (a) A graphene sheet made of C atoms placed at the corners of hexagons forming the lattice with arrows AA and ZZ denoting the rolling direction of the sheet to make (b) a (5,5) armchair nanotube and (c) a (10,0) zigzag nanotube	10
2.3 (a) Zig-Zag Single-Walled Nanotube. Note the zig-zag pattern around circumference and $m = 0$. (b) Chiral Single-Walled Nanotube. Note twisting of hexagons around tubule body. (c) Armchair Single-Walled Nanotube.	12
2.4 Schematic illustrations of the structures of (A) armchair, (B) zigzag, and (C) chiral SWNTs. Projections normal to the tube axis and perspective views along the tube axis are on the top and bottom, respectively. (D) Tunneling electron microscope image showing the helical structure of a 1.3-nm-diameter chiral SWNT. (E) Transmission electron microscope (TEM) image of a MWNT containing a concentrically nested array of nine SWNTs. (F) TEM micrograph showing the lateral packing of 1.4-nm-diameter SWNTs in a bundle. (G) Scanning electron microscope (SEM) image of an array of MWNTs grown as a nanotube forest.	13
2.5 Diagram showing rolling direction of nanotube	14
2.6 Structures of carbon nanotubes	15
2.7 Different structures of MWNTs. Top-left: cross-section of a MWNT the different walls are obvious, they are separated by 0.34nm. Rotation around the symmetry axis gives us the MWNT. Top-right: Symmetrical or non-symmetrical cone shaped end caps of MWNTs. Bottom-left: A SWNT with a diameter of 1,2nm and a bundle of SWNTs covered with amorphous carbon. Bottom-right: A MWNT with defects. In point P a pentagon defect and in	16



point H a heptagon defect.

2.8	Schematic diagram of a catalytically grown carbon nanofiber.	23
2.9	High-resolution electron micrographs and schematic representation of carbon nanofibers with their graphite platelets, (a) "perpendicular" and (b) "parallel" to the fiber axis.	24
2.10	Schematic diagram of arc-discharge apparatus.	28
2.11	Schematic drawings of a laser ablation apparatus.	29
2.12	TEM images of a bundle of SWNTs catalyzed by Ni/Y (2:0.5wt %) Mixture, produced with a continuous laser	30
2.13	Schematics drawings of a CVD deposition oven.	33
2.14	Schematic diagram of a vapour phase growth apparatus	35
2.15	Schematic diagram of thermal CVD apparatus	45
2.16	Schematic diagram of spurting machine	46
2.17	Schematic diagram of Plasma Enhanced CVD apparatus	48
2.18	Schematic diagram of the fluidized-bed reactor	49
2.19	Results of the mechanical properties from MWNT-polymer (epoxy) composites. (a) SEM micrograph that shows good dispersion of MWNTs in the polymer matrix. The tubes are, however, elastically bent due to their highly flexible nature. Schematic of an elastically bent nanotube is shown in (b). The strain is concentrated locally near the bend. (c) Stress-strain relationship observed during the tension/compression testing of the nanotube-epoxy (5 wt% MWNTs) composite (the curve that shows larger slope, both on the tension and compression sides of the stress-strain curve, belongs to the nanotube epoxy composite). It can be seen that the	54

load transfer to the nanotube is higher during the compression cycle (seen from the deviation of the composite curve from that of the pure epoxy), because in tension the individual layers of the nanotubes slide with respect to each other. (d) TEM image of a thicker straight MWNT as well as a buckled MWNT in an epoxy matrix after loading. The smaller diameter nanotubes have more tendencies to bend and buckle

- | | | |
|------|--|----|
| 2.20 | Results of mechanical properties measurements on SWNT-polymer composites. (a) SEM micrograph that shows a partially fractured surface of a SWNT-epoxy composite, indicating stretched nanotubes extending across cracks. (b) Shows a similar event illustrating the stretching and aligning of SWNT bundles across a long crack in SWNT-carbon soot composite. (c) SEM micrograph that shows the surface of a fractured SWNT-epoxy composite where the nanotube ropes have been completely pulled out and have fallen back on the fractured surface, forming a loose random network of interconnected ropes. (d) Shows results of micro-Raman spectroscopy that detects peak-shifts (in wave numbers) as a function of strain. In both tension and compression of the SWNT-epoxy specimens, the peak shifts are negligible, suggesting no load transfer to the nanotubes during the loading of the composites. | 57 |
| 2.21 | Shows significant pullout of the nanotubes from the matrix. | 62 |
| 2.22 | Two electrodes contact a single semi-conducting nanotube. The Si substrate, which is covered by a layer of SiO ₂ 300 nm thick, acts as a back-gate | 69 |
| 2.23 | The Samsung 4.5" full-color nanotube display | 71 |
| 2.24 | Schematic structure of nanotube flat panel display | 72 |
| 2.25 | Schematic representation of the helical of proteins crystallization on the outer surface of a carbon nanotube. | 75 |
| 2.26 | Schematic diagram of the carbon nanotube array biosensor. The enzyme immobilization allows for the direct electron transfer from the enzyme to platinum | 76 |

transducer were obtained with a JEOL-JSM 840 scanning microscope at 10 KV. Subsequently, enzyme immobilization was achieved by incubation for 3 h of both freshly oxidized sensors in an enzymatic solution (1500 to 2500 U/mL)

2.27	SEM images of the Pt-aligned carbon nanotube array (A) in original state, (B) after being chemically etched with a mixture of concentrated H ₂ SO ₄ and HNO ₃ acids (3:1, 98% and 65% respectively) for 8 h at 40 °C, washed with deionized water and dried at 100 °C overnight, and (C) after air oxidation at 600 °C for 5 min under air flow. SEM images were obtained with a JEOL-JSM 840 scanning microscope at 10KV. <i>Bar is 1 μm</i>	77
2.28	Use of a MWNT as AFM tip. VGCF stands for Vapour Grown Carbon Fibre. At the centre of this fibre the MWNT forms the tip	79
2.29	The AFM tip touches a single CNT in an attempt to pick it up	79
2.30	This image shows the comparison resolution between conventional tip and carbon nanotube tip	80
2.31	Temperature-dependent behavior of desorption of hydrogen	81
3.1	Schematic diagram of modified FC-CVD	85
3.2	Photo of experimental apparatus of FC-CVD	86
3.3	Flow chart of design and verification of FC-CVD	87
3.4	Flow chart of the optimization experiments	91
3.5	A photo of SEM JEOL 6400 at Microscopy & Microanalysis Unit in Institute of Bioscience, Universiti Putra Malaysia (UPM).	93
3.6	A photo of TEM Hitachi H-7100 at Microscopy &	94

3.7	Photo of TGA-7.	95
3.8	Schematic of Test Specimen used to find the Young's modulus of a composite	98
3.9	Flow chart of using carbon nanotube and carbon nanofiber as nanofiller with natural rubber (SMR CV60)	100
4.1	The outer diameter distribution of carbon nanotubes at different hydrogen flow rate: 50-500 ml/min (the other CVD parameters are fixed at reaction temperature= 800 °C and reaction time= 30 min).	108
4.2	Average diameter of CNTs at different hydrogen flow rate	110
4.3	Purity Of CNTs at different Hydrogen flow rate.	111
4.4	DTGA curve for three different samples	113
4.5	SEM images of (a) $R_T=500$ °C, $HF= 300$ ml/min and $R_t=45$ minute (b) $R_T=800$ °C, $HF= 300$ ml/min and $R_t=45$ minute and (c) $R_T=600$ °C, $HF= 300$ ml/min and $R_t=45$ minute.	114
4.6	The characteristics of deposited carbon material with hydrogen flow rate on the reactor tube wall, ceramic boat and their sum.	115
4.7	Yield of CNTs at different Hydrogen flow rate.	116
4.9	SEM Images of carbon nanotubes at (a) 50. (b) 100. (c) 150 (d) 200 (e) 250 (f) 300 (g) 350 (h) 400 (i) 450 and (j) 500 ml/min	119
4.10	TEM images of carbon nanotubes. (a) 50 (b) 100 (c) 150 (d) 200 (e) 250 (f) 300 (g) 350 (h) 400 (i) 450 and (j) 500 ml/min H_2 flow rate.	122

4.11	Scheme diagram of the effect of hydrogen gas on the activation of the surface catalyst and the decomposition of hydrocarbon on the active site of the surface	125
4.12	Average diameter of CNTs at different Hydrogen flow rate	127
4.13	The weight of deposited carbon material with reaction times on the reactor tube wall, ceramic boat and their sum.	128
4.14	Yield of CNTs at different Reaction Time.	129
4.15	The outer diameter distribution of carbon nanotubes at different Reaction temperature: 550-850 °C (the other CVD parameters are fixed at hydrogen flow rate= 300 ml/min and reaction time= 45 min).	134
4.16	The effect of reaction temperature on the average diameters of (a) CNTs (b) CNFs and (c) VGCFs	136
4.17	Purity of CNTs at different reaction temperature	137
4.18	The weight of deposited carbon material with different reaction temperature on the reactor tube wall, ceramic boat and their sum.	139
4.19	Yield of Carbon materials at different reaction temperature.	141
4.20	SEM Images of carbon nanotubes at (a) 550 °C. (b) 600 °C. (c) 650 °C (d) 700 °C (e) 750 °C (f) 850 °C and nanofibers at (g) 900 °C (h) 950 °C (i) 1000 °C	144
4.21	Vapor grown carbon fiber at (a) 1050 °C and (b) 1100 °C	147
4.22	Schematic diagram for adhering iron particles on the surface carbon fibers	147
4.23	(a) A net work carbon fiber (b) Branched carbon fiber	148

4.24	Schematic representation of different types of carbon fiber growth.	149
4.25	(a) and (b) is a scanning electron micrograph of the broken end of a thick VGCF	149
4.26	TEM images of carbon nanotubes at (a) 550 °C (b) 600 °C (c) 650 °C (d) 700 °C (e) 750 °C (f) 850 °C and carbon nanofibers at (g) 900 °C (h) 950 °C and (i) 1000 °C	153
4.27	Structure of carbon nanofiber (a) low magnification of TEM image (b) high magnification of TEM (c) another type of nanofiber	154
4.28	Schematic representation of the change in the size and the shape of the catalyst from (a) CNT to (b) CNF	156
4.29	A scheme is shown of the growth model for VGCF	157
4.30	Structure of CNTs (a) 800 °C (b) 850 °C and (c) 750 °C	158
4.31	Thermogravimetric (TG) curve as red colour Derivative thermogravimetric (DTG) curve as blue colour for pure CNTs	162
4.32	First order kinetics plot for CNTs at heating rate 10 °C/min	162
4.33	Stress-strain of SMR CV60 with different percentage of CNTs	167
4.34	Shows maximum strain (a) and stress (b) values at different wt % of CNTs	169
4.35	Young Modulus of SMR CV60 at different percentage of CNTs	171
4.36	Shows the toughness as function of wt % of CNTs	173

- 4.37 TEM image of CNTs in SMR CV60 (a) 1% wt of CNTs (b) 3 175
% wt of CNTs (c) 5 % wt of CNTs (d) 7 % wt of CNTs and
(e) 10 % wt of CNTs
- 4.38 Stress-strain of SMR CV60 with different percentage of 177
CNFs
- 4.39 Maximum stress and Strain values at different % of CNFs 179
- 4.40 Young Modulus of SMR CV60 at different percentage of 180
CNFs.
- 4.41 Toughness of the nanocomposite as function of wt % of 182
CNFs
- 4.42 TEM image of CNFs in SMR CV60 (a) 1% wt of CNFs (b) 3 184
% wt of CNFs (c) 5 % wt of CNTs (d) 7 % wt of CNFs and
(e) 10 % wt of CNFs